Vanadium Hydridotris(pyrazolyl)borate Complexes of Diphenyl Phosphate. Homometallic Trimeric Complexes of the $[LV\{(PhO)_2PO_2\}_3]^-$ Fragment

Norman S. Dean,[1a] Ladd M. Mokry,[1a] Marcus R. Bond,[1b] C. J. O'Connor,[1c] and Carl J. Carrano*,[1a]

Departments of Chemistry, Southwest Texas State University, San Marcos, Texas 78666, and University of New Orleans, New Orleans, Louisiana 70148

Received January 10, 1996[⊗]

The synthesis and characterization of two linear trinuclear V(III) complexes are described: **1**, $[LV(\mu\text{-}(PhO)_2PO_2)_3\text{-}V\text{-}(\mu\text{-}(PhO)_2PO_2)_3VL]PF_6$, and **2**, $LV(\mu\text{-}(PhO)_2PO_2)_2(\mu\text{-}OH)V(\mu\text{-}(PhO)_2PO_2)_2(\mu\text{-}OH)VL]ClO_4$, where L = hydridotris(pyrazolyl)borate. Compound **1** consists of two terminal V(III) ions capped by a hydridotris(pyrazolyl)borate group and each linked to a central V(III) by three (μ-O, μ-O′) diphenyl phosphate bridges. The structure of **2** is analogous but with a hydroxide bridge replacing a diphenyl phosphate in each link. X-ray crystal structural analysis of **1** and **2** gave the following parameters: **1**, $C_{98}H_{92}B_2F_6N_{16}O_{24}P_7V_3$, $P\bar{1}$, $a = 14.191(6)$ Å, $b = 14.338(4)$ Å, $c = 14.471(3)$ Å, $\alpha = 76.41(3)°$, $\beta = 71.10(3)°$, $\gamma = 81.22(2)°$, $Z = 1$, $V = 2698.3(15)$ Å^3; **2**, $C_{70}H_{68}B_2ClN_{14}O_{22}P_4V_3$, $P2_1/n$, $a = 13.035(5)$ Å, $b = 17.280(4)$ Å, $c = 19.343(8)$ Å, $\beta = 109.18(2)°$, $Z = 2$, $V = 4115(2)$ Å^3. Magnetic measurements indicate that replacement of one phosphate bridge with a hydroxide leads to a change in the sign of the coupling between the terminal and central V(III) atoms from antiferromagnetic (AF) in **1** to ferromagnetic (FM) in **2**. The similarity in structure between **2** and the previously reported $[L_2V_2(\mu\text{-}(PhO)_2PO_2)_2(\mu\text{-}OH)]ClO_4$ allows a comparison between their magnetic properties and confirms the previously postulated idea that the crossover from AF to FM coupling comes near a bridge angle of 133°.

Introduction

The rational[1] design and synthesis of new materials has been a long range goal of scientists for many years. The technological uses for these new materials are numerous and include shape selective catalysts, nonlinear and other electrooptic devices, high temperature superconductors, and high performance ceramics just to name a few. In most of these attempts organic chemistry has been at the forefront. This is because organic materials are generally viewed as more amenable to structural variation than their inorganic counterparts due to the wealth of synthetic transformations available. On the other hand the application of inorganic chemistry to the study of materials is undergoing a recent renaissance and it is becoming clear that the number of structural motifs available is large and growing rapidly. Thus the rest of the periodic table represents a huge and relatively untapped resource if only rational synthetic approaches to solid state materials can be developed. Previous attempts at rational synthesis of new inorganic materials has taken several routes. Among these include various supramolecular assembly methods,[2] including host−guest chemistry, and hydrothermal synthesis in the presence of templates.[3−5] Despite the development of these self-assembly methods, the more straightforward approach of rationally synthesizing small molecular building blocks which can be used as precursors for the formation of higher order structures under conventional conditions has lagged.

Vanadium phosphates make an interesting starting point for the testing of this approach. We were originally attracted to them because of the biological implications of vanadium−phosphate interactions.[6] Nevertheless vanadium phosphates have received most of their attention because of their unusual properties in the extended solid. Layered metal organophosphonates in particular have found applications as size-selective inorganic hosts, catalyst supports, and ion exchangers.[7−9] A wide variety of vanadium phosphate containing materials have been synthesized. Recently Zubieta and others have successfully exploited hydrothermal synthetic techniques to obtain a wealth of anionic cluster and layered oxovanadium organophosphates and phosphonates that arise from a complex and incompletely understood chemistry, and an extensive review is now available.[10]

In an attempt to rationally prepare polynuclear vanadium phosphate complexes from well-defined precursors, we have recently reported the synthesis of a series of trinuclear species of the formula $L_2V_2L'_6M$, where L = tris(pyrazolyl)borate, L′ = diphenyl phosphate, and M can be a mono-, di-, or trivalent metal ion.[11,12] In this paper we present the synthesis of the homometallic species where M = V(III) and where L′ can be diphenyl phosphate or hydroxide. We also report a study of the magnetic interactions between the metal ions which may have important implications with regard to the potential use of such linear trimers in the design of new molecular magnetic materials.

⊗ Abstract published in *Advance ACS Abstracts,* May 1, 1996.

(1) (a) Southwest Texas State University. (b) University of New Orleans. (c) Present address: Department of Chemistry, Southeast Missouri State University, Cape Girardeau, MO 63701.
(2) Muller, A.; Reuter, H.; Dillinger, S. *Angew. Chem, Int. Ed. Engl.* **1995**, *34*, 2328.
(3) Soghomonian, V.; Haushalter, R. C.; Chen, Q.; Zubieta, J. *Inorg. Chem.* **1994**, *33*, 700.
(4) Huan, G.; Day, V. W.; Jacobson, A. J.; Goshorn, D. P. *J. Am. Chem. Soc.* **1991**, *113*, 3188.
(5) Chen, Q.; Zubieta, J. *Angew. Chem., Int. Ed. Engl.* **1993**, *32*, 261.
(6) Toney, J. H.; Marks, T. J. *J. Am. Chem. Soc.* **1985**, *107*, 947.
(7) Johnson, D. C.; Jacobson, A. J.; Butler, W. M.; Rosenthal, S. E.; Brody, J. F.; Lewandowski, J. T. *J. Am. Chem. Soc.* **1989**, *111*, 381.
(8) Centi, G.; Trifiro, F.; Edner, J. R.; Francetti, V. M. *Chem. Rev.* **1988**, *88*, 55.
(9) Khan, M. I.; Lee, Y.; O'Connor, C. J.; Haushalter, R. C.; Zubieta, J. *Inorg.Chem.* **1994**, *33*, 3855.
(10) Khan, M. I.; Zubieta, J. In *Progress in Inorganic Chemistry*; John Wiley and Sons, Inc.: New York, 1995; pp 1−150.
(11) Mokry, L. M.; Thompson, J.; Bond, M. R.; Otieno, T.; Mohan, M.; Carrano, C. J. *Inorg. Chem.* **1994**, *33*, 2705.
(12) Dean, N. S.; Bond, M. R.; Mohan, M.; Mokry, L. M.; Carrano, C. J. Manuscript in preparation.

S0020-1669(96)00023-7 CCC: $12.00

Table 1. Crystallographic Data and Data Collection Parameters for **1** and **2**

parameter	**1**	**2**
formula	$C_{98}H_{92}B_2F_6N_{16}O_{24}P_7V_3$	$C_{70}H_{68}B_2ClN_{14}O_{22}P_4V_3$
space group	*P*1	$P2_1/n$
temp, K	173	298
a, Å	14.191(6)	13.035(5)
b, Å	14.338(4)	17.280(4)
c, Å	14.471(3)	19.343(8)
α, deg	76.41(3)	90.
β, deg	71.10(3)	109.18(2)
γ, deg	81.22(2)	90.
V, Å^3	2698.3(15)	4115(2)
ρ_{calc}, g cm^{-3}	1.467	1.445
Z	1	2
fw	2383.1	1791.2
cryst size, mm	0.4 × 0.2 × 0.4	0.2 × 0.3 × 0.2
μ, cm^{-1}	0.447	0.523
radiation	graphite-monochromated Mo Kα (λ = 0.710 73 Å)	
scan type	$\theta-2\theta$	$\theta-2\theta$
data collection range, deg	3.5−45	3.5−45
R_{merge}, %	n/a	6.87
no. of unique data	5506	5299
no. of obsd data, $F > 4.0\sigma(F)$	3655	2852
data:param ratio	5.2:1	5.2:1
transm min/max	XABS	0.351/0.479
R,[a] %	5.92	6.21
R_w,[a] %	7.22	6.65
max diff peak, e/Å^3	0.49	0.47
Δ/σ(mean)	0.007	0.003

[a] Quantity minimized $w(F_o - F_c)^2$. $R = \sum|F_o - F_c|/wF_o$. $R_w = (w(F_o - F_c)^2/\sum(wF_o)^2)^{1/2}$.

Experimental Section

All synthetic procedures were carried out under an atmosphere of pure dry argon or nitrogen by utilizing standard Schlenk techniques. Subsequent workup was carried out in air unless otherwise noted. Solvents were distilled under nitrogen from the appropriate drying agents (CaH_2 or Na/benzophenone). DMF was Burdick and Jackson "distilled in glass" while all other materials were reagent grade or better and used as received. Potassium hydridotris(pyrazolyl)borate was synthesized according to the reported method,[13] as was $[HB(pz)_3]VCl_2$·DMF.[14]

[{HB(C$_3$N$_2$H$_3$)$_3$}$_2$V$_3${(PhO)$_2$PO$_2$}$_6$](PF$_6$) (1). $[HB(pz)_3]VCl_2$·DMF (0.814 g, 2.0 mmol) and $Na[(PhO)_2PO_2]$ (1.632 g, 6.0 mmol) were added to a 200-mL Schlenk flask. CH_3CN (50−60 mL) was added, and the mixture was heated to reflux during which time it became blue-green in color. The reaction was stirred for $^1/_2$ h and allowed to cool, and then $NaPF_6$ (0.167 g, 1.0 mmol) was added. VCl_3·3THF (0.354 g, 1.0 mmol) was dissolved in 25 mL of CH_3CN and transferred to the reaction mixture. The flask was brought to reflux a second time and allowed to react for an additional 2 h. A gray-green precipitate formed in the reaction and was removed by filtration. The filtrate was then allowed to evaporate under a flow of dry nitrogen gas. X-ray quality crystals of complex **1** were obtained by allowing the filtrate to slowly evaporate at room temperature over 3 days. Yield: 1.12 g (50%). Anal. Calcd for **1**: C, 48.58; H, 3.62; N, 7.55. Found: C, 48.68; H, 3.76; N, 7.50. IR (cm^{-1}): 2500, 1588, 1488, 1405, 1238, 1200, 1094, 955. UV−vis, λ (ϵ): 570 nm (22), 706 nm (13).

[{HB(C$_3$N$_2$H$_3$)$_3$}$_2$V$_3${(PhO)$_2$PO$_2$}$_4$(OH)$_2$](ClO$_4$) (2). $[HB(pz)_3]$-VCl_2·DMF (0.814 g, 2.0 mmol) and $Na[(PhO)_2PO_2]$ (1.089 g, 4.0 mmol) were added to a Schlenk flask. CH_3CN (40 mL) was added, and the reaction mixture was brought to refluxing temperature and then allowed to cool. After 1 h, VCl_3·3THF (0.354g, 1.0 mmol) was added to the reaction vessel and the mixture again brought to reflux. After an additional 30 min NaOH (0.080 g, 2.0 mmol) was added to the reaction mixture along with 1.5 mL of degassed H_2O. The reaction mixture was allowed to stir for 8 h, producing a green/brown solution. $NaClO_4$ (0.140 g, 1.0 mmol) was added to the reaction, and the contents of the flask were stirred for an additional hour. The reaction was filtered under nitrogen, and a red/brown filtrate was obtained. The volume of the filtrate was reduced by 25% under a flow of dry nitrogen gas and left at room temperature. Over a period of 24 h, red crystals of complex **2** formed. *Caution!* all metal perchlorates are potentially hazardous. Yield: 0.97 g (55%). Anal. Calcd for **2**·CH_3CN: C, 46.67; H, 3.74; N, 10.40. Found: C, 46.30; H, 3.86; N, 10.59. IR (cm^{-1}): 2525, 1589, 1487, 1406, 1309, 1203, 1100, 848, 772, 691, 660, 619. UV−vis, λ (ϵ): 520 nm (113), 662 nm (51).

Physical Measurements. Routine infrared spectra were obtained on a Perkin-Elmer 1600 FT-IR as KBr pellets. UV−vis spectra were recorded on an HP 8520 diode array spectrophotometer. Paramagnetic NMR spectra were obtained in $CDCl_3$ solution on a Bruker NR-80 80 Mz FT-NMR spectrometer. Electrochemical and magnetic susceptibility measurements were made as previously described.[15,16]

Crystallography. Crystals were either attached to a glass fiber (low temperature, compound **1**) or sealed in a Lindeman glass capillary (room temperature, compound **2**) and mounted on a Siemens P4 diffractometer. Unit cell constants were determined by least squares refinement of the angular settings of 12−30 well-centered high-angle reflections. Structure solution and refinement were achieved using the SHELXTL-PLUS crystallography software from Siemens.[17] Pertinent parameters regarding crystal data, data collection, and structure solution and refinement are summarized in Table 1. In each case structure solution was achieved via direct methods, and subsequent structure refinement proceeded normally. Anisotropic thermal parameters were refined for all non-hydrogen atoms. Positions of the hydrogen atoms were calculated to give an idealized geometry and then fixed to ride on their respective bound atoms except for the position of the hydrogen bound to boron which was in each case located on the difference map and fixed through the remaining cycles of refinement. A fixed isotropic thermal parameter (0.08 Å^2) was assigned to each hydrogen. Atomic coordinates for **1** and **2** are listed in Tables 2 and 3, respectively, with pertinent bond lengths and angles given in Tables 4 and 5.

(13) Trofimenko, S. *J. Am. Chem. Soc.* **1967**, *89*, 3170.
(14) Mohan, M.; Holmes, S. M.; Butcher, R. J.; Jasinski, J. P.; Carrano, C. J. *Inorg. Chem.* **1992**, *31*, 2029.
(15) Bonadies, J. A.; Carrano, C. J. *J. Am. Chem. Soc.* **1986**, *108*, 4088.
(16) O'Connor, C. J. *Prog. Inorg. Chem.* **1982**, *29*, 203.
(17) Sheldrick, G. M. SHELXTL-PC, Version 4.1. Siemens X-Ray Analytical Instruments, Inc.; Madison, WI, 1989. Scattering factors from: *International Tables for X-Ray Crystallography*; Ibers, J., Hamilton, W., Eds.; Kynoch: Birmingham, U.K., 1974; Vol. IV.

Table 2. Atomic Coordinates ($\times 10^4$) and Equivalent Isotropic Displacement Coefficients ($Å^2 \times 10^3$) for **1**

	x	*y*	*z*	*U*(eq)[a]
V(1)	5000	5000	5000	17(1)
V(2)	3197(1)	6506(1)	2770(1)	18(1)
P(1)	2925(2)	4635(1)	4740(1)	20(1)
P(2)	3865(2)	7148(1)	4508(1)	20(1)
P(3)	4564(2)	4620(1)	7414(1)	20(1)
O(1)	4505(4)	5794(3)	2313(3)	22(1)
O(2)	2716(4)	5457(3)	3967(3)	20(1)
O(3)	3990(4)	4362(	4755(3)	15(1)
O(4)	2511(4)	3742(3)	4558(3)	23(1)
O(5)	2294(4)	4796(3)	5814(3)	22(1)
O(6)	3744(4)	7190(3)	3509(3)	23(1)
O(7)	4021(4)	6193(3)	5140(3)	19(1)
O(8)	3894(4)	7731(3)	5041(4)	28(1)
O(9)	4771(4)	7729(3)	4402(3)	24(1)
O(10)	4452(4)	4487(3)	6460(3)	18(1)
O(11)	4420(4)	5740(3)	7390(3)	25(1)
O(12)	3706(4)	4135(4)	8327(3)	31(1)
B(1)	1891(8)	7551(7)	1303(7)	29(1)
N(1)	2674(5)	5901(4)	1870(4)	24(1)
N(2)	2124(5)	6466(4)	1288(4)	24(1)
C(1)	2798(6)	5016(5)	1663(5)	27(1)
C(2)	2342(7)	5009(6)	966(5)	33(1)
C(3)	1944(6)	5926(6)	732(5)	31(1)
N(3)	3576(5)	7613(4)	1515(4)	23(1)
N(4)	2901(5)	7989(4)	996(4)	25(1)
C(4)	4384(7)	8108(5)	1075(5)	27(1)
C(5)	4230(7)	8819(5)	295(6)	28(1)
C(6)	3305(7)	8731(5)	258(6)	38(1)
N(5)	1789(5)	7232(4)	3119(4)	27(1)
N(6)	1341(5)	7637(4)	2388(5)	30(1)
C(7)	1145(7)	7422(6)	3969(6)	37(1)
C(8)	274(7)	7937(6)	3822(6)	47(1)
C(9)	450(7)	8054(6)	2807(6)	39(1)
C(11)	2432(6)	2101(5)	4675(6)	35(1)
C(12)	2373(7)	1164(6)	5206(7)	55(1)
C(13)	2373(7)	936(6)	6183(8)	54(1)
C(14)	2420(7)	1663(6)	6657(7)	54(1)
C(15)	2504(7)	2607(6)	6122(6)	46(1)
C(16)	2485(6)	2806(5)	5137(6)	32(1)
C(21)	515(7)	4694(6)	6066(5)	31(1)
C(22)	−454(7)	5097(6)	6346(6)	41(1)
C(23)	−662(7)	5981(6)	6624(6)	43(1)
C(24)	116(7)	6466(6)	6619(6)	39(1)
C(25)	1085(6)	6071(5)	6354(5)	27(1)
C(26)	1286(6)	5190(5)	6059(5)	25(1)
C(31)	1650(7)	8446(5)	6264(6)	36(1)
C(32)	1289(7)	8661(6)	7214(6)	43(1)
C(33)	1856(7)	8363(6)	7880(6)	47(1)
C(34)	2769(7)	7875(6)	7588(6)	44(1)
C(35)	3139(7)	7659(6)	6658(6)	37(1)
C(36)	2579(7)	7947(5)	5994(6)	28(1)
C(41)	5468(6)	8636(5)	2771(5)	27(1)
C(42)	5690(7)	9528(6)	2127(6)	42(1)
C(43)	5394(8)	10366(6)	2496(7)	52(1)
C(44)	4839(7)	10336(6)	3508(6)	46(1)
C(45)	4621(7)	9458(5)	4143(6)	35(1)
C(46)	4942(6)	8627(5)	3753(5)	24(1)
C(51)	5469(6)	6868(5)	7410(6)	30(1)
C(52)	5864(7)	7325(6)	7939(6)	38(1)
C(53)	5586(7)	7086(6)	8980(6)	43(1)
C(54)	4931(7)	6387(6)	9503(6)	36(1)
C(55)	4539(6)	5922(5)	8971(5)	25(1)
C(56)	4820(6)	6164(5)	7941(5)	24(1)
C(61)	2204(8)	3558(7)	8387(6)	52(1)
C(62)	1160(8)	3726(8)	8517(7)	72(1)
C(63)	686(8)	4594(9)	8629(6)	73(1)
C(64)	1162(8)	5341(8)	8631(6)	57(1)
C(65)	2159(7)	5189(7)	8520(6)	41(1)
C(66)	2640(7)	4315(6)	8403(5)	37(1)
P(4)	0	0	0	91(1)
F(1)	66(7)	−19(5)	1077(5)	127(1)
F(2)	65(7)	1131(5)	−271(6)	123(1)
F(3)	1181(6)	−181(6)	−370(6)	121(1)
N(71)	15511(1)	1124(9)	3154(9)	162(1)
C(71)	2048(9)	467(8)	2934(7)	79(1)
C(72)	2629(9)	−388(7)	2721(8)	81(1)
N(72)	3102(8)	1456(7)	68(8)	96(1)
C(73)	2305(10)	1719(8)	419(8)	77(1)
C(74)	1266(8)	2097(10)	862(8)	113(1)

[a] Equivalent isotropic *U* defined as one-third of the trace of the orthogonalized $\mathbf{U}_{ij}$ tensor.

Table 3. Atomic Coordinates ($\times 10^4$) and Equivalent Isotropic Displacement Coefficients ($Å^2 \times 10^3$) for **2**

	x	*y*	*z*	*U*(eq)[a]
V(1)	0	0	5000	28(1)
V(2)	362(1)	−1396(1)	3709(1)	31(1)
P(1)	1923(2)	570(1)	6497(1)	33(1)
P(2)	932(2)	428(1)	3696(1)	33(1)
O(1)	−1246(4)	−1219(3)	3366(3)	34(1)
O(2)	534(4)	−963(3)	4671(3)	30(1)
O(3)	1452(4)	133(3)	5805(3)	35(1)
O(4)	2222(5)	−42(3)	7142(3)	43(1)
O(5)	3093(4)	894(3)	6586(3)	40(1)
O(6)	597(5)	−339(3)	3328(3)	37(1)
O(7)	553(4)	620(3)	4322(3)	34(1)
O(8)	537(5)	1052(3)	3066(3)	40(1)
O(9)	2212(4)	505(3)	4002(3)	38(1)
B(1)	1446(9)	−2962(7)	3387(6)	49(2)
N(1)	1993(5)	−1707(4)	4078(3)	37(2)
N(2)	2311(6)	−2415(5)	3875(4)	48(2)
C(1)	2906(7)	−1375(6)	4511(5)	49(2)
C(2)	3805(8)	−1843(6)	4585(5)	63(2)
C(3)	3379(8)	−2497(7)	4186(6)	65(2)
N(3)	367(6)	−1833(4)	2710(4)	41(2)
N(4)	839(6)	−2533(4)	2675(4)	47(2)
C(4)	−65(9)	−1566(6)	2029(5)	61(2)
C(5)	120(9)	−2106(7)	1533(5)	79(2)
C(6)	684(9)	−2695(6)	1972(5)	68(2)
N(5)	63(6)	−2534(4)	3950(3)	37(2)
N(6)	597(6)	−3141(4)	3765(4)	46(2)
C(7)	−658(8)	−2851(5)	4230(5)	50(2)
C(8)	−576(8)	−3651(6)	4243(5)	59(2)
C(9)	201(8)	−3795(5)	3941(5)	58(2)
C(11)	1778(8)	−219(6)	8224(5)	55(2)
C(12)	1925(9)	−33(7)	8943(5)	69(2)
C(13)	2649(9)	511(7)	9307(5)	77(2)
C(14)	3222(10)	896(8)	8949(6)	103(2)
C(15)	3127(9)	713(7)	8231(5)	79(2)
C(16)	2369(7)	175(5)	7873(4)	42(2)
C(21)	3832(8)	2158(6)	6596(5)	55(2)
C(22)	4035(8)	2792(6)	6227(6)	69(2)
C(23)	3673(8)	2816(6)	5479(6)	66(2)
C(24)	3121(7)	2192(6)	5083(5)	59(2)
C(25)	2894(7)	1569(6)	5455(5)	50(2)
C(26)	3276(7)	1548(5)	6199(5)	40(2)
C(31)	465(8)	2257(5)	3695(5)	54(2)
C(32)	745(9)	3028(6)	3808(6)	70(2)
C(33)	1376(10)	3366(7)	3453(7)	93(2)
C(34)	1734(9)	2954(7)	2966(7)	84(2)
C(35)	1437(8)	2168(6)	2826(6)	66(2)
C(36)	827(7)	1846(5)	3212(4)	42(2)
C(41)	4053(7)	412(5)	4095(5)	48(2)
C(42)	4839(8)	280(6)	3784(5)	63(2)
C(43)	4575(9)	108(6)	3054(6)	71(2)
C(44)	3489(9)	74(6)	2616(5)	58(2)
C(45)	2674(8)	199(5)	2914(4)	46(2)
C(46)	2980(7)	366(5)	3661(4)	36(2)
N(7)	1929(8)	8189(6)	5911(5)	85(2)
C(51)	2398(8)	8104(7)	6500(6)	66(2)
C(52)	2984(9)	8013(7)	7258(5)	97(2)
C1(2)[b]	927(5)	163(4)	680(3)	76(2)
O(21)[b]	768(12)	424(12)	1271(8)	116(2)
O(22)[b]	1975(11)	36(10)	801(7)	94(2)
O(23)[b]	607(21)	−468(15)	605(19)	352(2)
O(24)[b]	374(18)	659(12)	27(13)	190(2)

[a] Equivalent isotropic *U* defined as one-third of the trace of the orthogonalized $\mathbf{U}_{ij}$ tensor. [b] Occupancy factors for Cl(2), O(21), O(22), O(23), and O(24) are 0.500.

Results

Synthesis. Complex **1** was synthesized from a two-step reaction. In the first stage of the preparation, $[HB(pz)_3]VCl_2 \cdot DMF$ and $Na[(PhO)_2PO_2]$ were reacted in CH_3CN to form *in situ* the species $[HB(pz)_3]V[(PhO)_2PO_2]_3^-$. This was then reacted further with $^1/_2$ equiv of $VCl_3 \cdot 3THF$, in the presence of $NaPF_6$, to form the trinuclear V(III) species.

Complex **2** was first isolated and crystallographically characterized as a minor product from a reaction of $[HB(pz)_3]VCl_2 \cdot DMF$ and $Na[(PhO)_2PO_2]$ with $La(ClO_4)_3$. A rational route to **2** has been developed employing a modification of the

Table 4. Bond Lengths (Å) and Angles (deg) for **1**

V(1)−O(3)	1.975(6)	V(1)−O(7)	2.038(5)
V(1)−O(10)	1.997(4)	V(1)−O(3A)	1.975(6)
V(1)−O(7A)	2.038(5)	V(1)−O(10A)	1.997(4)
V(2)−O(1)	1.967(5)	V(2)−O(2)	2.013(4)
V(2)−O(6)	1.991(6)	V(2)−N(1)	2.087(8)
V(2)−N(3)	2.093(5)	V(2)−N(5)	2.071(7)
O(3)−V(1)−O(7)	89.2(2)	O(3)−V(1)−O(10)	89.7(2)
O(7)−V(1)−O(10)	89.8(2)	O(3)−V(1)−O(3A)	180.0(1)
O(7)−V(1)−O(3A)	90.8(2)	O(10)−V(1)−O(3A)	90.3(2)
O(3)−V(1)−O(7A)	90.8(2)	O(7)−V(1)−O(7A)	180.0(1)
O(10)−V(1)−O(7A)	90.2(2)	O(3A)−V(1)−O(7A)	89.2(2)
O(3)−V(1)−O(10A)	90.3(2)	O(7)−V(1)−O(10A)	90.2(2)
O(10)−V(1)−O(10A)	180.0(1)	O(3A)−V(1)−O(10A)	89.7(2)
O(7A)−V(1)−O(10A)	89.8(2)	O(1)−V(2)−O(2)	92.7(2)
O(1)−V(2)−O(6)	90.7(2)	O(2)−V(2)−O(6)	93.1(2)
O(1)−V(2)−N(1)	89.1(3)	O(2)−V(2)−N(1)	92.8(2)
O(6)−V(2)−N(1)	174.2(2)	O(1)−V(2)−N(3)	91.0(2)
O(2)−V(2)−N(3)	175.2(3)	O(6)−V(2)−N(3)	89.8(3)
N(1)−V(2)−N(3)	84.3(3)	O(1)−V(2)−N(5)	173.9(3)
O(2)−V(2)−N(5)	89.5(2)	O(6)−V(2)−N(5)	94.9(3)
N(1)−V(2)−N(5)	85.1(3)	N(3)−V(2)−N(5)	86.4(2)

Table 5. Bond Lengths (Å) and Angles (deg) for **2**

V(1)−O(2)	1.987(6)	V(1)−O(3)	2.030(5)
V(1)−O(7)	2.002(6)	V(1)−O(2A)	1.987(6)
V(1)−O(3A)	2.030(5)	V(1)−O(7A)	2.002(6)
V(2)−O(1)	2.002(5)	V(2)−O(2)	1.949(5)
V(2)−O(6)	2.030(6)	V(2)−N(1)	2.080(7)
V(2)−N(3)	2.077(8)	V(2)−N(5)	2.087(8)
O(2)−V(1)−O(3)	90.2(2)	O(2)−V(1)−O(7)	89.9(2)
O93)−V(1)−O(7)	89.8(2)	O(2)−V(1)−O(2A)	180.0(1)
O(3)−V(1)−O(2A)	89.8(2)	O(7)−V(1)−O(2A)	90.1(2)
O(2)−V(1)−O(3A)	89.8(2)	O(3)−V(1)−O(3A)	180.0(1)
O(7)−V(1)−O(3A)	90.2(2)	O(2A)−V(1)−O(3A)	90.2(2)
O(2)−V(1)−O(7A)	90.1(2)	O(3)−V(1)−O(7A)	90.2(2)
O(7)−V(1)−O(7A)	180.0(1)	O(2A)−V(1)−O(7A)	89.9(2)
O(3A)−V(1)−O(7A)	89.8(2)	O(1)−V(2)−O(2)	92.2(2)
O(1)−V(2)−O(6)	90.5(2)	O(2)−V(2)−O(6)	91.0(2)
O(1)−V(2)−N(1)	173.7(3)	O(2)−V(2)−N(1)	89.3(2)
O(6)−V(2)−N(1)	95.6(3)	O(1)−V(2)−N(3)	94.0(3)
O(2)−V(2)−N(3)	173.4(3)	O(6)−V(2)−N(3)	86.7(3)
N(1)−V(2)−N(3)	84.8(3)	O(1)−V(2)−N(5)	88.0(3)
O(2)−V(2)−N(5)	96.9(3)	O(6)−V(2)−N(5)	172.0(2)
N(1)−V(2)−N(5)	85.7(3)	N(3)−V(2)−N(5)	85.6(3)

synthesis of complex **1**. In this case $[HB(pz)_3]VCl_2 \cdot DMF$ and $Na[(PhO)_2PO_2]$ are reacted in a 1:2 ratio in CH_3CN. Following the addition of the $VCl_3 \cdot 3THF$, a stochiometric amount of NaOH is added along with a small amount of water. After several hours of stirring, $NaClO_4$ is added to provide the desired counterion.

Description of Structures. The structure of $[\{HB(C_3N_2H_3)_3\}_2V_3\{(PhO)_2PO_2\}_6](PF_6)$ consists of the linear trinuclear cationic V(III) species, a PF_6 counterion, and two CH_3CN solvent molecules. The structure and atom-labeling scheme of the cationic portion of the molecule are shown in Figure 1. The molecule is sitting on a crystallographically imposed inversion center, resulting in the PF_6 anion being located in two positions with 50% occupancy. The cationic trinuclear species is composed of three V(III) atoms each bridged by three η_1:η_1 diphenyl phosphate ligands. The central vanadium atom is nearly octahedral with an average V−O bond distance of 2.003 Å. Coordination of the terminal vanadium atoms is completed by a tris(pyrazolyl)borate ligand, (average V−N distance 2.084 Å). The large bite angle of the bridging phosphates results in a terminal to central vanadium−vanadium distance of 4.691Å, well outside of the range for any possible metal−metal bonding.

The structure of $[\{HB(C_3N_2H_3)_3\}_2V_3\{(PhO)_2PO_2\}_4(OH)_2](ClO_4)$ consists of the linear trinuclear cationic V(III) species,

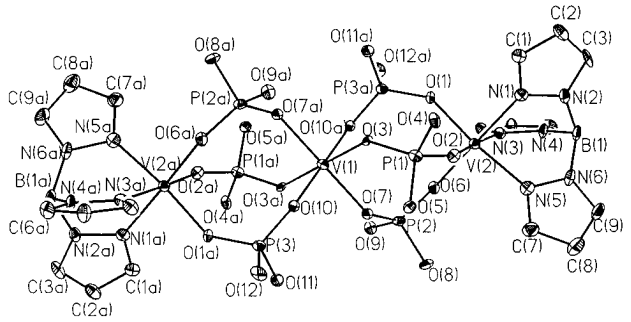

Figure 1. Thermal ellipsoid plot (30%) showing the atom-labeling scheme for the non-carbon atoms of the cationic portion of **1**. Phenyl rings have been omitted for clarity.

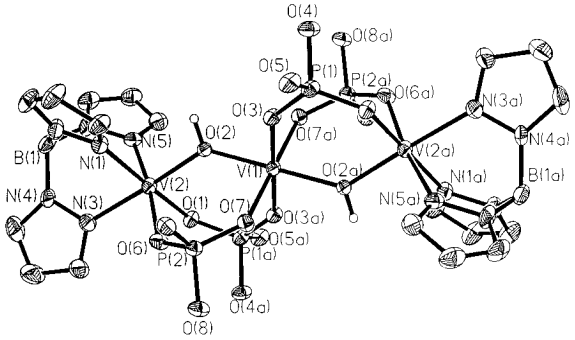

Figure 2. Thermal ellipsoid plot (30%) showing the atom-labeling scheme for the non-carbon atoms of the cationic portion of **2**. Phenyl rings have been omitted for clarity.

a ClO_4 counterion, and two CH_3CN solvent molecules. The overall structure and atom-labeling scheme for the cationic portion are outlined in Figure 2. The molecule again spans a crystallographically imposed inversion center so that the ClO_4 anion is forced into two positions with 50% occupancy. The cationic linear trinuclear complex contains three vanadium(III) atoms. The central metal atom is bound to four η_1:η_1 bridging diphenyl phosphates and two bridging hydroxide ligands. The presence of the inversion center necessitates that the hydroxide ligands be in the "anti" arrangement. The coordination of the central vanadium atom is nearly octahedral with the V−OH bond distances of 1.987 Å and V−OP bond distances averaging 2.016 Å. The coordination of the terminal vanadium atoms is again completed by a facially capping tris(pyrazolyl)borate ligand. The average V−N distances in the complex show little trans influence of the bridging hydroxide. V−N bond lengths trans to the hydroxide are 2.077 Å while the V−N bond lengths trans to the bridging phosphate oxygens average 2.084 Å. The V−O−V angle at the bridging hydroxide is 133.2(3)°, with the vanadium−vanadium separation between the terminal and central vanadium(III) atoms being a reasonably close 3.612 Å.

Magnetic Measurements. Variable temperature magnetic susceptibility data were collected in the temperature range of 2−300 K for both **1** and **2**. An empirical diamagnetic correction was derived from a plot of susceptibility versus inverse temperature and applied to the data for **1**. The diamagnetic correction for **2** was made using Pascal's constants.[18] The magnetic moment for **1** remains essentially constant throughout most of the temperature range before decreasing rapidly below 50 K. No peak in the susceptibility curve was noted. The data was analyzed using the HDVV (Heisenberg−Dirac−Van Vleck) spin Hamiltonian for a linear trimer (eq 1) where $S_1 = S_2 = S_3 = 1$, corrected for weak secondary interactions using the molecular field approach.[16]

(18) Carlin, R. L. *Magnetochemistry*; Springer-Verlag: Berlin, 1986.

$$\begin{matrix} A\text{--}A\text{--}A \\ S_1 \quad S_2 \quad S_3 \end{matrix}$$

$$H_{exch} = -2[J_{12}\cdot S_1\cdot S_2 + J_{23}\cdot S_2\cdot S_3 + J_{13}\cdot S_1\cdot S_3] \qquad (1)$$

This gave excellent fits to the data (Figure 3) with parameters $g = 1.675(3)$, $J_{12} = -2.70(2)$ cm^{-1}, and $zJ'/k = -0.721(8)$ K with J_{13} set to zero. Not surprisingly, the data could be fit equally well with two coupling constants, one for the adjacent coupling (J_{12}) and another for the terminal (J_{13}). However, the two constants were highly correlated and summed to the value obtained above so that there appeared to be no mathematical justification for the extra parameter. Accordingly, as is commonly done,[19] the terminal coupling, J_{13}, was fixed at zero. Very different magnetic behavior was noted for **2**, where one of the bridging phosphate ligands was replaced by hydroxide. In this case the magnetic moment again remained fairly constant from 300 to about 100 K when it began to have a pronounced upturn and reached a maximum at about 10 K before falling again below this temperature. This is indicative of moderate *intra*trimer ferromagnetic coupling with either weak antiferromagnetic *inter*trimer coupling and/or single ion zero field splitting. Fits to the data (Figure 4) were again excellent employing equation 1 and including a molecular field correction as well as one for TIP which gave $g = 1.709(2)$, $J_{12} = +9.5(2)$ cm^{-1}, $zJ'/k = -0.0621(8)$ K, and TIP $= 0.0004$. As before, fits to the two coupling constants were mathematically unjustified, and J_{13} was again fixed at zero.

Electrochemistry. Within the potential window available on Pt electrodes in acetonitrile solution both **1** and **2** show two equal current reductive cyclic voltammetric waves (Figure 5). For **1** these waves overlap and appear at -0.89 and -1.02 V (vs $Ag/AgNO_3$), while in **2** they are distinct and occur at -1.00 and -1.20 V. All these reductive waves can be classified as quasireversible based on a ΔE_p of 65−90 mv (70 mv for ferrocene) and an i_{pa}/i_{pc} near 1.0. The difference in potential between the two reductive waves is 135 mV for **1** and 200 mv for **2**.

Paramagnetic NMR. The electronic relaxation properties of V(III) complexes of the type reported here are often favorable for the observation of relatively sharp paramagnetically shifted NMR spectra. As expected **1** shows three well-resolved paramagnetically shifted resonances at -20.1, $+2.0$, and $+10.2$ ppm assigned as the H3, H5, and H4 protons respectively on the tris(pyrazolyl)borate rings. The assignments are based on comparison to previously reported μ-phosphato−V(III) dimers.[20] The observation of only three resonances confirms the 3-fold cylindrical symmetry expected of **1** based on its solid state structure. Assuming a simple π delocalization pathway for the unpaired electron density, an alternating sign pattern around the aromatic pyrazolyl ring is expected[21] and is indeed observed in the analog where a diamagnetic Ba ion occupies the central position. However in **1** there is a change in the sign of the shift for H5 such that the alternating sign pattern is lost, suggesting a change to a σ-dominated delocalization mechanism. In **2** the situation is more complex with nine distinct resonances observed clustered in three separate groups ($+17.4$, $+16.1$, and $+14.4$ ppm), ($+9.4$, $+8.0$, and $+7.6$ ppm), and (-9.7, -11.4, and -12.7 ppm). It is difficult to unequivocally assign all these resonances without selective deuteration but it is clear that unexpectedly, based on the solid state structure, solution **2** has less than 2-fold symmetry, rendering all three pyrazole rings inequivalent.

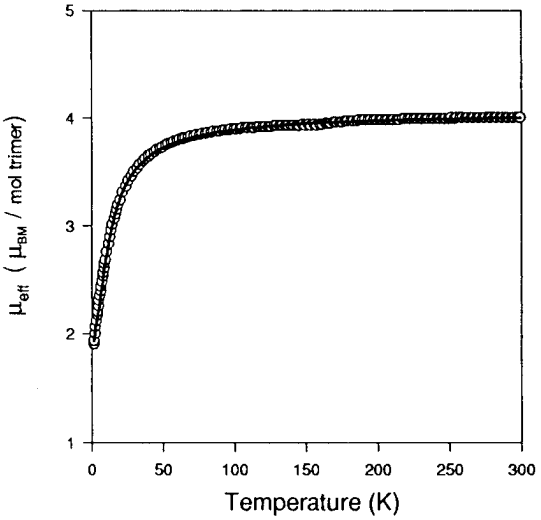

Figure 3. Plot of χT vs T for **1**. The open circles are the data while the solid line represents the nonlinear least-squares fit to that data using the model and parameters presented in the text.

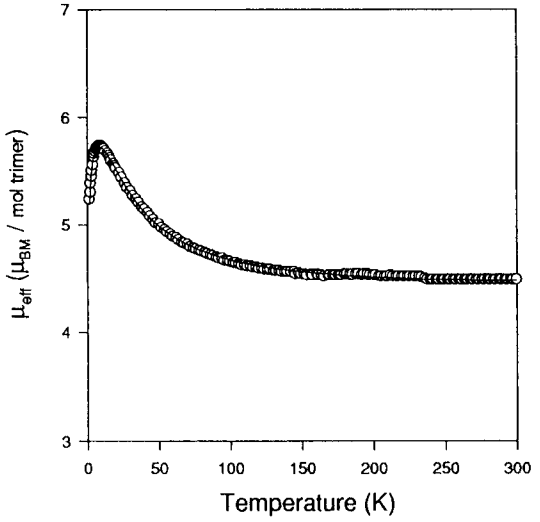

Figure 4. Plot of χT vs T for **2**. The open circles are the data while the solid line represents the nonlinear least-squares fit to that data using the model and parameters given in the text.

Discussion

We have previously presented the synthesis of a series of neutral trinuclear heterometallic vanadium complexes containing the $HB(pz)_3V((PhO)_2PO_2)_3^-$ fragment where the vanadium phosphate unit serves as a strong chelating agent for M^{2+} ions.[12] Structural characterization of these species was accomplished for a variety of M^{2+} species (Ca, Ba, Mg, Mn) and synthetic methods were presented for a number of other transition metal containing species (i.e. Fe,Co, Ni).[12] While complexation of metals in other than the $+2$ oxidation state was achieved for monovalent Na and trivalent Al and La, structural verification of these complexes or other charged trinuclear species was elusive. Suspecting that at least a portion of the difficulties in obtaining crystalline material might be due to scrambling of the heterometal among the terminal and central positions, we attempted the synthesis of the homometallic V(III) analog.

The synthesis of the V_3 complex was accomplished from a reaction analogous to that used to produce the M^{2+} species.

(19) Kessissoglou, D. P.; Kirk, M. L.; Lah, M. S.; Li, X.; Raptopoulou, C.; Hatfield, W. E.; Pecoraro, V. L. *Inorg. Chem.* **1992**, *31*, 5424.
(20) Bond, M. R.; Czernuszewicz, R. S.; Dave, B. C.; Yan, Q.; Mohan, M.; Verastegue, R.; Carrano, C. J. *Inorg. Chem.* **1995**, *34*, 5857.
(21) Swift, T. J. In *NMR of Paramagnetic Molecules; Principles and Applications*; La Mar, G. N., Ed.; Academic Press: New York, 1973.

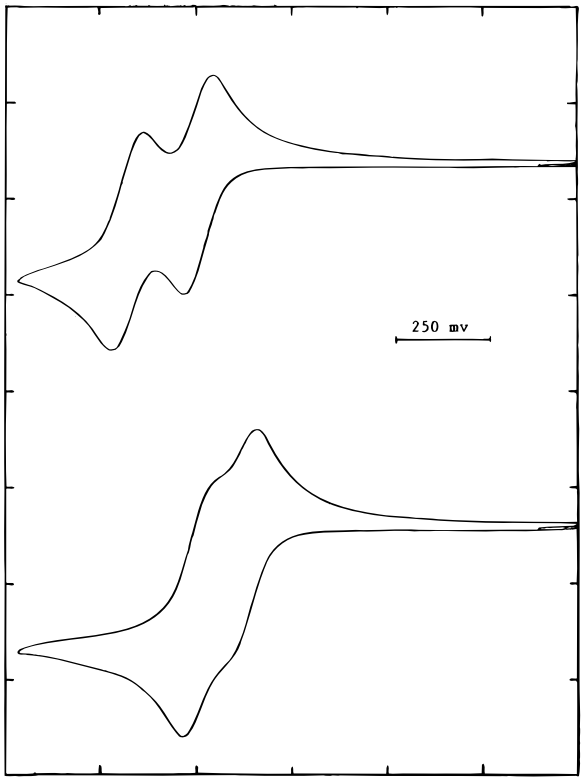

Figure 5. Cyclic voltammetry of a 5 mg/mL solution of **1** (lower) and **2** (upper) in acetonitrile at a scan rate of 100 mV/s.

$LVCl_2$·DMF and 3 equiv of $Na[(PhO)_2PO_2]$ are reacted in CH_3CN under refluxing conditions. Previously we have shown that this reaction produces $HB(pz)_3V((PhO)_2PO_2)_3^-$, which can be isolated as the Na^+ salt. Addition of $^1/_2$ equiv of VCl_3·3THF provides the third metal ion for formation of the trinuclear species, while $NaPF_6$ was provided as a source of the counterion. Unlike the neutral species which precipitate from the CH_3CN solvent, the cationic trinuclear species are soluble in CH_3CN and are isolated, after filtration of NaCl, by slow evaporation of the solvent.

The structure of complex **1** consists of a linear arrangement of three vanadium(III) atoms each bridged by three diphenyl phosphates. The terminal metal to central metal distance of 4.691 Å is well outside of the range for any possible metal−metal bonding. The average metal to phosphate oxygen bond length is essentially identical for both metal positions (1.990 Å terminal vs 2.004 Å central) consistent with all three metals being in the +3 oxidation state. The average vanadium nitrogen bond distance for the terminal metals is 2.084 Å. The bridging phosphates all show an O−P−O bridging bond angle of approximately 119°. These structural parameters can be compared to those found in the case of the M^{2+} trimers. The best comparison is to the Mn complex, as it has the atomic radius closest to vanadium(III). In the Mn complex the vanadium to bridging phosphate oxygen distances are similar but slightly shorter at 1.952 Å while the average vanadium−nitrogen distance is increased to 2.115 Å. However, the most striking effect is the lengthening of the central metal to phosphate oxygen distance by 0.2 Å to 2.203 Å. This is consistent with the decreased Coulomb interactions expected on going from a M^{3+} to a M^{2+} ion. As a result of this increase in bond length there is a corresponding increase in the O−P−O angle to 122.2° and an increase in the central to terminal metal distance to 4.761 Å.

Various other structural changes occur on replacing a bridging phosphate ligand in **1** with a bridging hydroxide as in **2**. First, the metal−hydroxide oxygen bond lengths for the terminal and central vanadiums are inequivalent at 1.949 and 1.987 Å, respectively, and slightly shorter than those found for the phosphate ligands, suggesting some multiple bond character. We attribute the longer bonds around the latter to be due to a weak "trans effect" since the hydroxides are trans to each other on the central metal and therefore compete for the same metal orbital while they are trans to a (pyrazolyl)borate nitrogen for the terminal ones. Second, the V−O−V bridging angle of 133.2° results in a drastic decrease in the vanadium−vanadium separation to 3.612 Å. While this distance is still outside of the range for direct metal metal bonding it is well within the range for which significant magnetic coupling might be expected to be mediated by the bridging hydroxide ligand. The decreased metal-metal separation also forces a slight contraction of the O−P−O bridging angles to 117.0°. These bonding parameters are very similar to those seen in the previously reported dimeric analog,[20] $V_2(OH)(O_2P(OC_6H_5)_2)_2(HBpz_3)_2$, which has V−OH bonds of 1.959 Å and a V−O−V angle of 133.1°. Similar Fe- and Mn-containing linear trimers with acetate rather than phosphate bridges are also known.[22,23]

Electrochemically, two types of limiting behavior might be anticipated for reduction of a homometallic linear trimer. If the two symmetry-related terminal metals are both reduced at the same potential (i.e. the noninteracting limit) with the central metal reducing at some different potential, then two waves should be observed in the cyclic voltammetry, with the wave corresponding to the terminal metals having twice the current of the one for the central metal. If on the other hand there is communication between the two terminal metals such that they reduce independently, then three distinct one-electron waves could be observed with the separation (ΔE) between the two waves corresponding to the terminal metals dependent on the degree of interaction between them.[24] The observation of only two closely spaced reductive waves, *but with the same current*, for both **1** and **2** is only consistent with their assignment as reductions of weakly interacting terminal V(III)'s. The central V(III) in an all oxygen environment is expected to reduce at a much more negative potential than the N_3O_3-coordinated terminal metals and is apparently outside the potential window observable on Pt in acetonitrile. This assignment is further confirmed by the observation of two closely spaced waves at similar potentials to those seen for **1** and **2** in the complex where the central V(III) has been replaced by the redox inactive Al(III). The increased ΔE found in **2** vs **1** indicates a greater interaction between metals in the former consistent with both the shorter through space distance between terminal metals in **2** and the greater efficiency of hydroxide vs phosphate as a ligand in mediating magnetic superexchange.

The magnetic differences between **1** and **2** are intriguing given that the two complexes differ only in the replacement of one anionic diphenyl phosphate ligand for a hydroxide ion. In a previous publication we have reported that the diphenyl phosphate group supports only a weak antiferromagnetic exchange coupling (AFC), on the order of −4 K, in some structurally related bis(μ-phosphato)-bridged V(III) dimers.[25] Assuming no coupling between the terminal metals, the magnitude of the weak AFC seen in **1** is very similar despite

(22) Kitajima, N.; Osawa, M.; Imai, S.; Fujisawa, K.; Moro-oka, Y.; Heerwegh, K.; Reed, C. A.; Boyd, P. D. *Inorg. Chem.* **1994**, *33*, 4613.
(23) Kitajima, N.; Amagai, H.; Tamura, N.; Ito, M.; Moro-oka, Y.; Heerwegh, K.; Penicaud, A.; Mathur, R.; Reed, C. A.; Boyd, P. D. *Inorg. Chem.* **1993**, *32*, 3583.
(24) Coe, B. J.; Meyer, T. J.; White, P. S. *Inorg. Chem.* **1995**, *34*, 3600.
(25) Dean, N. S.; Mokry, L. M.; Bond, M. R.; O'Connor, C. J.; Carrano, C. J. *Inorg Chem.*, in press.

the fact that the two vanadium centers are bridged by three rather than only two phosphates. When a phosphate ligand is switched with a hydroxide (a ligand expected to promote better exchange), we arrive at a structure that is analogous to the the previously reported, dimer, $V_2(OH)(O_2P(OC_6H_5)_2)_2(HBpz_3)_2$. In discussing the magnetism of this latter complex, we have proposed, based on a simple molecular orbital approach, that the exchange coupling would change from AF to FM once the bridge angle reached a value beyond which the difference in orbital energy is less than the cost in spin pairing energy.[20] In fact the vanadium atoms in the μ-hydroxo−bis(μ-phosphato) dimer, where the bridge angle is 133°, are more FM coupled (i.e. essentially uncoupled) than the corresponding carboxylate-bridged complex where the angle is 120° and $J = -37$ K. The observation of weak FMC in **2** where the angle is a bit over 133° is entirely consistent with this view and indicates clearly that the crossover point between FM and AF coupling must lie very near a bridge angle of 133°.

Acknowledgment. C.J.C. wishes to thank Prof. W. E. Geiger for useful discussions concerning the electrochemistry and the Robert A. Welch foundation through Grant AI-1157, the Dreyfus Foundation, and the NIH through AREA Grant GM4767601 for partial support of this work. The NSF-ILI program Grant USE-9151286 is also acknowledged for support of the X-ray diffraction facilities at SWTSU.

Supporting Information Available: Complete lists of atomic positions, bond lengths and angles, anisotropic displacement parameters, hydrogen atom coordinates, and data collection and crystal structure parameters for **1** and **2** (22 pages). Ordering information is given on any current masthead page.

IC9600238